International Journal of Control and Automation
Vol.9, No.3 (2016), pp.215-226
http://dx.doi.org/10.14257/ijca.2016.9.3.20

Image Processing of Remote Sensor using Lifting Wavelet and Curvelet Transform

Hong Zhong

Gannan Normal University, Ganzhou, China
gnsyzh@126.com

Abstract

Nowadays, Geographic Information System (GIS) has been widely used in traffic control or urban planning and monitoring, thus, remote sensing images should be processed in digital form, which allows rapid integration of remote sensing analysis into a GIS. This paper discusses an image processing approach by using lifting wavelet and curvelet transform to carry out the image fusion of remote sensing photos. This approach integrates the lifting wavelet and curvelet transform to deal with the challenges in remote sensing image fusion. Experiments are carried out for testing the feasibility and compare the proposed approach with traditional wavelet manner. The experimental results show that, the correlation coefficients of primary low waveband from the proposed model are a little bit higher than the panchromatic waveband. That implies the image fusion can be performed better by the proposed model. Additionally, it was found that, the enhancement of information entropy will be improved by 7.73% and 9.84% respectively from both two experiments.

Keywords*: Image Processing, Remote Sensor, Lifting Wavelet, Curvelet Transform.*

1. Introduction

Nowadays, Geographic Information System (GIS) has been widely used in traffic control or urban planning and monitoring [1]. Remote sensing could be provided undoubtedly through using the satellites. By using the GIS, we are able to access the remote sensing images for different purposes [2]. However, such images should be processed in digital form, which allows rapid integration of remote sensing analysis into a GIS [3-5]. For processing the remote sensor image, there are several challenges. Images from remote sensing are very complex due to the image information formed without making physical contact with the object and thus in contrast to in situ observation [6]. Such images may include lots of noises and it is very challenging to restore the reality of the non-physical touched objects. Secondly, the remote sensing images are usually very large. That means they are carrying enormous information which is difficult to address using traditional image processing algorithms or models. Finally, there are different types of remote sensor techniques such as radar, film photography, infrared and radiometers. Take hyperspectral imaging for example, an image is very sophisticated that each pixel has full spectral information with imaging narrow spectral bands over s contiguous spectral range [7]. As a result, processing these images is very hard.

In order to address the above challenges, large number of studies has been carried out. For the remote sensing images about Earth from space took by the satellites, [8] proposed an approach to get rid of the statistical characterization of remote sensing images rather than in gray scale natural images. This book illustrates the remote sensing image processing by five main parts: remote sensing, image processing, computer vision, signal processing, and machine learning. Remote sensing images need to be converted into tangible information. To this end, an object-based method was proposed to delineate

ISSN: 2005-4297 IJCA

readily usable object from imagery so as to utilize spectral and contextual information in an integrative way [9]. From this paper, it could be found that cracks and the OBIA (Object Based Image Analysis) methods are making significant progress towards a spatially explicit information extraction workflow. Using unmanned aircraft system as a remote sensing platform, an automated batch processing method based on the object image was used to derive a species-level vegetation classification [10]. It is observed that, using this methodology, the overall accuracy has been improved by 87%. From the literature, most of the studies focus on the classification of remote sensing images [11-16]. Image fusion on the remote sensing photos is limited.

The lifting scheme for the construction of bi-orthogonal wavelets has been proposed by Wim Sweldens [17]. The lifting wavelet features that all constructions are derived in the spatial domain, which is based on simple mathematical calculations. Lifting scheme is a simple and efficient algorithm to calculate the wavelet transforms to generate second-generation wavelets that could be used for the image fusion. There are three steps for constructing wavelets based on the lifting scheme. (1) Split phase: split data into odd and even sets; (2) predict phase: odd set is predicted from even set; (3) update phase: update even set using wavelet coefficient to calculate scaling function.

This method is used to improve a given discrete wavelet transform to obtain specific properties which suits the remote sensing image which has the above characteristics. However, the transform using lifting may cause large difference when carrying out in remote sensing image fusion because the discrete transforms will accumulate the lifting residual when generating the second-generations. In order to reduce the lifting residual, this paper integrates the curvelet transform into the lifting wavelet for implementing remote sensing image fusion.

The rest of this paper will be organized as follows. Section 2 gives a presentation about the lifting wavelet by giving the basic concept and integer change in lifting wavelet. Section 3 presents the curvelet transform. Section 4 introduces the proposed model by integrating lifting wavelet and curvelet transform. Experiments are also demonstrated in this section. Finally, section 5 concludes this paper and gives the future research directions.

2. Lifting Wavelet

2.1 Basic Concept

In the 1990s, Sweldens, Daubechies and Schroder introduced an approach using the lifting algorithm for constructing the dual orthogonal function [17]. The lifting wavelet uses linear, nonlinear, space-change based prediction, and update operator for lifting change. That ensures the reverse of change. The wavelet generated from such approach is named second-generation wavelet which is based on dual orthogonal wavelet and total restorable filter, aiming to improve the dualization. The following steps are the key phases in lifting wavelet:

(1) Split

Assume a signal $s=(s_k), k \in Z, s_k \in R$, s is divided into even sample $s_e=(s_{2k})$ and odd sample $s_o=(s_{2k+1})$. The decomposition is called lazy wavelet transform:

$$(s_e, s_o) = S(s_k) \qquad (1)$$

(2) Prediction

Since the samples from s have some relations, s_o could be estimated from s_e,

$$s_o = P(s_e) \qquad (2)$$

Where P is the prediction operator, which reflects the relation between the data. The difference between predicted value and real value reveals the degree of approximation from the prediction operator. The smaller the difference is the degree of approximation is better.

(3) Update

In order to totally reconstruct s, the information related to s_e included in s_o will be omitted. The difference between them could be reserved as $r = s_o - P(s_e)$. Using this approach, some characteristics from s maybe missed. Thus, the update operation is needed by using the new r to fine-tune the s_e:

$$\lambda = s_e + U(r) \tag{3}$$

The forward change of lifting wavelet could be expressed as:

$$\begin{cases} (s_e, s_o) = S(s_k) \\ r = s_o - P(s_e) \\ \lambda = s_e + U(r) \end{cases} \tag{4}$$

Where r and λ is the wavelet coefficient and scale coefficient in the multi-resolution analysis. S, P, and U are decomposition operator, prediction operator, and update operator respectively. If the decomposition change of the lifting wavelet is obtained, the reconstruction approach could be expressed as:

$$\begin{cases} s_e = \lambda - U(r) \\ s_o = \lambda + P(s_e) \\ s = M(s_e, s_o) \end{cases} \tag{5}$$

2.2 Integer Change in Lifting Wavelet

S transform is the integer form of Haar wavelet. For a integer sequence $\{s_j\}$, $s_{0,j} = s_j$, the Haar wavelet transform is

$$s_{1,l} = \frac{s_{0,2l} + s_{0,2l+1}}{2}, d_{1,l} = s_{0,2l+1} - s_{0,2l} \tag{6}$$

The reverse transform is

$$s_{0,2l} = s_{1,l} + d_{2,l} / 2, s_{0,2l+1} = s_{1,l} - d_{1,l} / 2 \tag{7}$$

The S transform could be obtained from using the integer from (7).

$$s_{1,l} = \left\lfloor \frac{s_{0,2l} + s_{0,2l+1}}{2} \right\rfloor, d_{1,l} = s_{0,2l+1} - s_{0,2l} \tag{8}$$

Since two integers' sum or difference is odd or even, the integerization operation removes the last unit from the sum is odd and it is equal to the last unit from the difference. Thus the S transform is reversal, the reverse of S transform is:

$$s_{0,2l} = s_{1,l} - \lfloor d_{2,l} / 2 \rfloor, s_{0,2l+1} = s_{1,l} - \lfloor (d_{1,l} + 1) / 2 \rfloor \tag{9}$$

In order to get better lifting, the forward and afterward difference calculations could be obtained as:

$$d_{1,l} = s_{0,2l+1} - s_{0,2l}, s_{1,l} = s_{0,2l} + d_{1,j} / 2 \quad (10)$$

$$s_{0,2l} = s_{1,l} - d_{1,j} / 2, s_{0,2l} - d_{1,j} / 2 \quad (11)$$

The integer transform is

$$d_{1,l} = s_{0,2l+1} - s_{0,2l}, s_{1,l} = s_{0,2l} + \lfloor d_{1,j} / 2 \rfloor \quad (12)$$

The reverse transform is

$$s_{0,2l} = s_{1,l} - \lfloor d_{1,j} / 2 \rfloor, s_{0,2l+1} = s_{0,2l} + d_{1,l} \quad (13)$$

Based on the S transform, we propose a TS approach for realize the integer lifting wavelet with the dual orthogonal wavelet basis from low filter coefficient $\{0.5, 0.5\}$ and high filter coefficient $\{0.125, 0.125, -1, 1, -0.125, -0, 125\}$. The TS transform is:

$$d_{1,l}^{(1)} = s_{0,2l+1} - s_{0,2l}, s_{1,l} = s_{0,2l} + d_{1,l}^{(1)} / 2 \quad (14)$$

$$d_{1,l} = d_{1,l}^{(1)} + s_{1,l-1} / 4 - s_{1,j+1} / 4 \quad (15)$$

The corresponding integer transforms are:

$$d_{1,l}^{(1)} = s_{0,2l+1} - s_{0,2l}, s_{1,l} = s_{0,2l} + \lfloor d_{1,l}^{(1)} / 2 \rfloor \quad (16)$$

$$d_{1,l} = d_{1,l}^{(1)} + \left\lfloor s_{1,l-1} / 4 - s_{1,j+1} / 4 + \frac{1}{2} \right\rfloor \quad (17)$$

While the reverse transforms are:

$$d_{1,l}^{(1)} = d_{1,l} - \left\lfloor s_{1,l-1} / 4 - s_{1,j+1} / 4 + \frac{1}{2} \right\rfloor \quad (18)$$

$$s_{0,2l+1} = d_{1,l}^{(1)} + s_{0,2l}, s_{0,2l} = s_{1,l} - \lfloor d_{1,l}^{(1)} / 2 \rfloor \quad (19)$$

From the above illustrations, the direct transform could be obtained:

$$d_{1,l}^{(1)} = s_{0,2l+1} - s_{0,2l}, s_{1,l} = s_{0,2l} + \lfloor d_{1,l}^{(1)} \rfloor \quad (20)$$

$$d_{1,l} = d_{1,l}^{(1)} + \lfloor \alpha_{-1}(s_{1,l-2} - s_{1,l-1}) + \alpha_0(s_{1,l-1} - s_{1,l}) + \alpha_1(s_{1,l} - s_{1,l+1}) - \beta_1 d_{1,l-1}^{(1)} \rfloor \quad (21)$$

Where $\alpha_{-1} = 0, \alpha_0 = 0.25, \alpha_1 = 0.75, \beta_1 = -0.25$.

3. Curvelet Transform

Assume the function $\psi : R \to R$ meets the condition: $\int \psi(t)dt = 0$ and the admissible condition $K_\psi = \int \frac{|\psi(w)|^2}{|w|^n} dw < \infty$. Then ψ is the admissible neural activation function under n space. For the parameter set $r = (a, u, b)$, define the

$R^n \to R$ function, then the $\psi_r = a^{-0.5}\psi(\frac{< a, x > -b}{a})$ is ridgelet. Where $r \in \Gamma$, Γ is the parameter space, $\Gamma = \{r = (a,u,b) : a,b \in R, u \in S^{n-1}\}$. S^{n-1} is the unit ball of R^n. a is the scale parameter, b is the position parameter, and u is the direction parameter.

Definition 1. Continuous Ridgley transform is $R(f)(r) =< f, \psi_r >$ and a function meets $\hat{f} \in L^1(R^n)$, if ψ satisfies the admissible condition, then

$$f = c_\psi \int < f, \psi_r > \psi_r(x) u(dr) \tag{22}$$

Where $c_\psi = \pi(2\pi)^{-n} K_\psi^{-1}$, $u(dr) \Rightarrow \frac{da}{a^{n+1}} dudb$.

Definition 2. Parseval Relation. Assume $f \in L^1(R^n) \cap L^2(R^n)$, ψ satisfies the admissible condition, then we can get:

$$\| f \|_2^2 = c_\psi \int | < f, \psi_r > |^2 \, u(dr) \tag{23}$$

From the above definition, the curvelet transform $R : L^2(R^n) \to L^2(\Gamma, u(d_r))$ is isometric mapping under L^2: $R(f)(r) =< f, \psi_r >$. For $\forall f \in L^2(R^n)$, the curvelet transform is equal to $R(f)(r) =< P_u f, \psi_{a,b} >$, where $\psi_{a,b} = a^{\frac{1}{2}} \psi(a(t-b))$.

4. Proposed Model for Remote Sensing Image Processing

4.1 Model Description

With the lifting wavelet and curvelet transform approach, this section presents a remote sensing image processing model which integrates lifting wavelet and curvelet transform to suit the characteristics of such image.

Definition 3. Under a space H which indicates a remote sensing image, a set of functions $\{\psi_r\}_{r \in \square}$, if $0 < A < B < \infty$, for $f \in H$, we can get:

$$A \| f \|^2 \le \sum_r | < f, \psi_r > |^2 \le B \| f \|^2 \tag{24}$$

Thus, $\{\psi_r\}_{r \in \square}$ is a frame in H, A, B are the boundary. Meanwhile, $\exists \hat{\psi}_r$ is the dual frame s.t.

$$f = \sum_{\lambda \in \Gamma_n} < f, \psi_r > \hat{\psi}_r = \sum_{\lambda \in \Gamma_n} < f, \hat{\psi}_r > \psi_r \tag{25}$$

According to the characteristics of wavelet transform, in the frequency domain, the supporting interval of curvelet transform is along with u direction. The discretion of scale and angle divides the two dimensional plane into multiply structures. For the remote sensing image processing, the proposed model follows several steps:

(1) Image classification based on odd and even indicator

According to the definitions, the classification is:

$$s_{1,l}^{(1)} = s_{1,2l}, d_{1,l}^{(0)} = s_{1,2l+1} \tag{26}$$

The dual lifting includes the application of a filter to get the even samples, which could be used for extracting the results using the following equation:

$$d_{1,l}^{(1)} = d_{1,l}^{(i-1)} - \sum_k p_k^{(i)} s_{l-k}^{(l-1)} \quad (27)$$

$$s_{1,l}^{(1)} = s_{1,l}^{(i-1)} - \sum_k u_k^{(i)} d_{l-k}^{(l-1)} \quad (28)$$

(2) Processing of the odd and even samples

For the M step dual lifting and primary lifting, the even samples are low filter coefficient and the odd samples are high filter coefficient. K is the scale indicator, thus, we can get:

$$s_{1,j} = s_{1,j}^{(M)} / K, d_{1,l} = K d_{1,l}^{(M)} \quad (29)$$

The reverse calculation is $s_{1,j}^{(M)} = K s_{1,j}, d_{1,l}^{(M)} = d_{1,l} / K$.

Then the M could be obtained, and the primary and dual lifting step could be alternatively got:

$$s_{1,l}^{(i-1)} = s_{1,l}^{(i)} + \sum_k u_k^{(i)} d_{1,l-k}^{(i)}, d_{1,l}^{(i-1)} = d_{1,l}^{(i)} + \sum_k p_k^{(i)} s_{1,l-l}^{(i-1)} \quad (30)$$

(3) Restore even and odd sample

The samples are restored by using the following expresses:

$$s_{0,2l} = s_{1,l}^{(0)}, s_{0,2l+1} = d_{1,l}^{(0)} \quad (31)$$

The proposed model with dual lifting and curvelet transform with the reverse transform is:

$$d_{1,l}^{(i)} = d_{1,l}^{(i-1)} - \left\lfloor \sum_k p_k^{(i)} s_{1,l-k}^{(i-1)} + \frac{1}{2} \right\rfloor \quad (32)$$

$$s_{1,l}^{(i)} = s_{1,l}^{(i-1)} - \left\lfloor \sum_k u_k^{(i)} d_{1,l-k}^{(i)} + \frac{1}{2} \right\rfloor \quad (33)$$

$$s_{1,l}^{(i-1)} = s_{1,l}^{(i)} - \left\lfloor \sum_k u_k^{(i)} d_{1,l-k}^{(i)} + \frac{1}{2} \right\rfloor \quad (34)$$

$$d_{1,l}^{(i-1)} = d_{1,l}^{(i)} - \left\lfloor \sum_k p_k^{(i)} s_{1,l-k}^{(i-1)} + \frac{1}{2} \right\rfloor \quad (35)$$

4.2 Experiments

The experiments are carried out by using the images from remote sensing images with colors. Two types of images are used for carrying out the experiments. In the first experiment, the original image comes from open wild area with the size of 203×203 pixels that from cameras from an airplane.

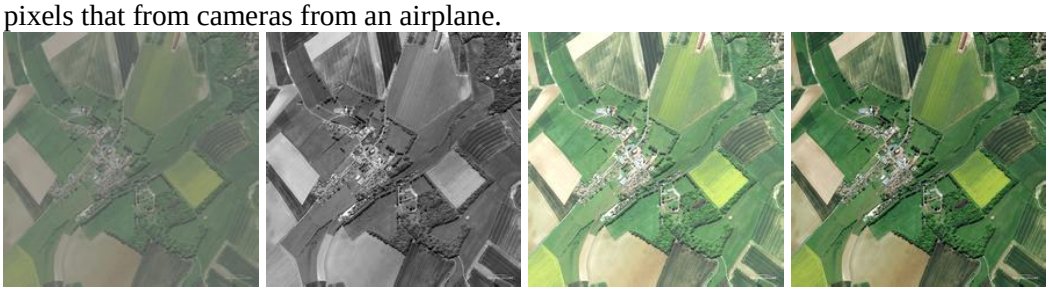

(a)Original image (b)Gray processing (c)Wavelet-based (d)Proposed Model

Figure 1.Experimental Results-1

(a) Original image (b) Wavelet manner (c) Proposed Model

Figure 2. Experimental Results-2

For the remote sensing image $n=2, a_0=2$, let ψ satisfies the curvelet. The ridgelet function of ψ is

$$\psi_{a,\theta,b} = a^{-1/2}\psi(\frac{x\cos\theta + y\sin\theta - b}{a}) \qquad (36)$$

$\psi_{a,\theta,b}$ has three parameters: a is the scale, θ is the angle and b is the position. The supporting set is $\{(x,y):|x\cos\theta + y\sin\theta| - b \le a\}$. For any square integral function f, the coefficient of curvelet is:

$$R_f(a,\theta,b) = < f, \psi_{a,\theta,b} > = \int f(x)\overline{\psi}_{a,\theta,b}(x)dx \qquad (37)$$

$\overline{\psi}$ is the conjugate complex number of ψ and has the total reconstruction formula:

$$f = \int_0^{2\pi}\int_{-\infty}^{+\infty}\int_0^{+\infty} R_f(a,\theta,b)\frac{da}{a^3}db\frac{d\theta}{4\pi} \qquad (38)$$

After the discrete of the three parameters, we can get:

$$\{\psi_{j,l,k}(x) = 2^{j/2}\psi(2^j(x_i\cos\theta_{j,l} + x_2\sin\theta_{j,l}) - k)\}_{j,k,l\in\square} \qquad (39)$$

(39) is a frame of L^2. According to the definition, $\forall f \in L^2, \exists A, B > 0$,

$$A\|f\|_{L^2}^2 \le \sum_{j,l,k} |< f, \psi_{j,l,k} >|^2 \le B\|f\|_{L^2}^2 \qquad (40)$$

Thus, f could be reconstructed by the curvelet coefficient set $\{< f, \psi_{j,l,k} >\}$. Based on the dual theory, there is a $\{\tilde{\psi}_{j,l,k}\}_{j,k,l\in\square}$ which is the dual set of $\{\psi_{j,l,k}\}_{j,k,l\in\square}$, s.t.

$$f = \sum_{j,l,k} < f, \psi_{j,l,k} > \tilde{\psi}_{j,l,k} = \sum_{j,l,k} < f, \tilde{\psi}_{j,l,k} > \psi_{j,l,k} \qquad (41)$$

This model uses the angle parameter θ for presenting the directions of pixels in remote sensor images. The discrete of θ is $\theta_{j,l} = 2\pi\theta_0 l 2^{-j}$.

From the qualitative analysis of (40) and (41), db4 is selected for carrying out the image fusion of remote sensing. The decomposition layer of lifting wavelet is one. Due to the wave phases are from the same sensor device, this experiment compares the traditional fusion approach – gray processing, the wavelet fusion with db4, and the

proposed model in this paper. Figure 1 (a) is an original image taken by a remote sensor equipment from a farm in Canada. Figure 1 (b) is an image that has been processed by traditional grayscale fusion approach which is a conversion of a color image to grayscale by different weighting of the color channels effectively represent the effect of shooting black-and-white film with different-colored photographic filters. This approach use the principles of photometry to match the luminance of the grayscale image to the luminance of the original color image. Figure 1 (c) is the image under processed by wavelet manner which uses the transform for imaging processing to implement the fusion of images. Figure 1 (d) is the results from the approach integrating with lifting wavelet and curvelet.

In order to test the feasibility and effectiveness of fusion of the remote sensing images, information entropy is proposed in this paper for this purpose. The entropy is the average amount of information from the image. We defined the image information entropy is:

$$H(X) = \sum_i P(x_i) I(x_i) = -\sum_i P(x_i) \log_b P(x_i) \tag{42}$$

Where X is an image, $P(x_i)$ is the probability mass function of a pixel in X. To do this, a continuous function f is used and it is discretized into bins of size Δ. Based on the mean value theorem, there will be a value x_i in each bin that

$$f(x_i)\Delta = \int_{i\Delta}^{(i+1)\Delta} f(x)dx \tag{43}$$

We denote that

$$H^{\Delta} := -\sum_{i=-\infty}^{\infty} f(x_i)\Delta \log(f(x_i)\Delta) \tag{44}$$

Using the expanding of the logarithm, we can get

$$H^{\Delta} := -\sum_{i=-\infty}^{\infty} f(x_i)\Delta \log(f(x_i)) - \sum_{i=-\infty}^{\infty} f(x_i)\Delta \log(\Delta) \tag{45}$$

As $\Delta \to 0$, we can have

$$\sum_{i=-\infty}^{\infty} f(x_i)\Delta \to \int_{-\infty}^{+\infty} f(x)dx = 1 \tag{46}$$

$$\sum_{i=-\infty}^{\infty} f(x_i)\Delta \log(f(x_i)) \to \int_{-\infty}^{+\infty} f(x) \log f(x)dx \tag{47}$$

Thus, we can finally get

$$h[f] = \lim_{\Delta \to 0}(H^{\Delta} + \log \Delta) = -\int_{-\infty}^{\infty} f(x) \log f(x)dx \tag{48}$$

From the above experiment, the information entropy from the images is shown in table 1.

Images	Correlation coefficient of panchromatic waveband	Correlation coefficient of primary low waveband	Information entropy

Figure 1 (a)	-	-	7.1382
Figure 1 (b)	-	-	6.1256
Figure 1 (c)	0.8666	0.8347	7.2854
Figure 1 (d)	0.8789	0.9864	7.8482
Figure 2 (a)	-	-	8.9878
Figure 2 (b)	0.7655	0.7898	9.1028
Figure 2 (c)	0.8868	0.9964	9.9988

From table 1, the correlation coefficients of panchromatic waveband and primary low waveband from different images are obtained. From the two experiments, the correlation coefficients of panchromatic waveband from Figure 1 (c) and (d) as well as Figure 2 (b) and (c) are 0.8666, 0.8789, 0.7655, and 0.8868. The ones from the model proposed in this paper is bigger than traditional wavelet approaches. For the correlation coefficient of primary low waveband, the differences are even obvious from the two experiments, which are 0.1517 and 0.2066 respectively. However, the differences of panchromatic waveband are 0.0123 and 0.1213. It is observed that, from the experiments, the correlation coefficients of primary low waveband from the proposed model are a little bit higher than the panchromatic waveband. That implies the image fusion can be performed better by the proposed model.

For illustrating the information entropy from table 1, Figure 1 (b) is the smallest value which means the grayscale operation will lose some information of the image from remote sensing. After the image fusion, the information entropy will be creased. That indicates that more information will be useful and reflected from the image which will be clearer. It could be found that, the proposed approach in this paper with lifting wavelet and curvelet transform outperforms the traditional wavelet approach used in image fusion. The enhancement of information entropy will be improved by 7.73% and 9.84% respectively from both two experiments.

5. Conclusion

This paper discusses an image processing approach by using lifting wavelet and curvelet transform to carry out the image fusion of remote sensing photos. This approach integrates the lifting wavelet and curvelet transform by three steps so as to deal with the challenges in remote sensing image fusion. Experiments are carried out in two dimensions to test the feasibility of the proposed model by comparing with the traditional wavelet approach used in image fusion. From the experiments, it could be observed that, the proposed methodology outperforms the traditional wavelet manner in terms of the correlation coefficients of panchromatic waveband and primary low waveband as well as the information entropy.

There are some limitations in this research so that future research directions could be implemented so as to improve this approach. First of all, the application of the proposed approach will be extended into other applicable areas such as biomedical image processing. The biomedical images are complex that high density of

information maybe hidden within an image. Secondly, the odd and even samples selected from this approach could be improved by adding some more selection methodologies such as stochastic manner. Finally, the wavelet calculation is very simple. It is easily attacked or decrypted by other unauthorized users. More sophisticated methods could be studied and added into the model for keeping more secure system.

References

[1]. M.F. Goodchild, "Geographic information system", in Encyclopedia of Database Systems, ed: Springer, **(2009)**, pp. 1231-1236.
[2]. E. Chuvieco, I. Aguado, M. Yebra, H. Nieto, J. Salas and M.P. Martín, "Development of a framework for fire risk assessment using remote sensing and geographic information system technologies", Ecological Modelling, vol. 221, **(2010)**, pp. 46-58.
[3]. R.Y. Zhong, Q.Y. Dai, K. Zhou and X.B. Dai, "Design and Implementation of DMES Based on RFID", Proceeding of 2nd International Conference on Anti-counterfeiting, Security and Identification, Guiyang, August **(2008)**, pp. 475-477.
[4]. J. Jenkins, S. Hartley, J. Carter, D. Johnson and J. Alford, "A geographic information system tool for aquatic resource conservation in the red and sabine river watersheds of the southeast united states", River Research and Applications, vol. 29, **(2013)**, pp. 99-124.
[5]. R.Y. Zhong, G.Q. Huang, S.L. Lan, Q.Y. Dai, C. Xu and T. Zhang, "A Big Data Approach for Logistics Trajectory Discovery from RFID-enabled Production Data", International Journal of Production Economics, vol. 165, **(2015)**, pp. 260-272.
[6]. S. Goetz and R. Dubayah, "Advances in remote sensing technology and implications for measuring and monitoring forest carbon stocks and change", Carbon Management, vol. 2, **(2011)**, pp. 231-244.
[7]. T.A. Akbar and S.R. Ha, "Landslide hazard zoning along Himalayan Kaghan Valley of Pakistan-by integration of GPS, GIS, and remote sensing technology", Landslides, vol. 8, **(2011)**, pp. 527-540.
[8]. R.Y. Zhong, G.Q. Huang, S. Lan, Q. Dai, T. Zhang and C. Xu, "A two-level advanced production planning and scheduling model for RFID-enabled ubiquitous manufacturing", Advanced Engineering Informatics, vol. doi:10.1016/j.aei.2015.01.002, **(2015)**.
[9]. R.Y. Zhong, Z. Li, A.L.Y. Pang, Y. Pan, T. Qu and G.Q. Huang, "RFID-enabled Real-time Advanced Planning and Scheduling Shell for Production Decision-making", International Journal of Computer Integrated Manufacturing, vol. 26, **(2013)**, pp. 649-662.
[10]. R.Y. Zhong, G.Q. Huang, Q.Y. Dai and T. Zhang, "Mining SOTs and Dispatching Rules from RFID-enabled Real-time Shopfloor Production Data", Journal of Intelligent Manufacturing, vol. 25, **(2014)**, pp. 825-843.
[11]. W. Zhang, L. Wang, D. Liu, W. Song, Y. Ma and P. Liu, "Towards building a multi-datacenter infrastructure for massive remote sensing image processing", Concurrency and Computation: Practice and Experience, vol. 25, **(2013)**, pp. 1798-1812.
[12]. R.Y. Zhong, Q.Y. Dai, T. Qu, G. J. Hu and G.Q. Huang, "RFID-enabled Real-time Manufacturing Execution System for Mass-customization Production", Robotics and Computer-Integrated Manufacturing, vol. 29, **(2013)**, pp. 283-292.
[13]. M.L. Wang, T. Qu, R.Y. Zhong, Q.Y. Dai, X.W. Zhang and J.B. He, "A radio frequency identification-enabled real-time manufacturing execution system for one-of-a-kind production manufacturing: a case study in mould industry", International Journal of Computer Integrated Manufacturing, vol. 25, **(2012)**, pp. 20-34.
[14]. L. Zhang, L. Zhang, D. Tao and X. Huang, "On combining multiple features for hyperspectral remote sensing image classification, Geoscience and Remote Sensing", IEEE Transactions, vol. 50, **(2012)**, pp. 879-893.
[15]. X. Qiu, H. Luo, G.Y. Xu, R.Y. Zhong and G.Q. Huang, "Physical Assets and Service Sharing for IoT-enabled Supply Hub in Industrial Park (SHIP)", International Journal of Production Economics, vol. 159, **(2014)**, pp. 4-15.
[16]. L.Y. Pang, R.Y. Zhong, J. Fang and G.Q. Huang, "Data-source interoperability service for heterogeneous information integration in ubiquitous enterprises", Advanced Engineering Informatics, vol. doi:10.1016/j.aei.2015.04.007, **(2015)**.
[17]. L. Pang, Z. Li, G.Q. Huang, R.Y. Zhong, Y. Pan and T. Qu, "Reconfigurable Auto-ID Enabled Software as a Service (SaaS) Shell for Real-Time Fleet Management in Industrial Parks", Journal of Computing in Civil Engineering, 10.1061/(ASCE)CP.1943-5487.0000306 , 04014032, **(2014)**.

Authors

Hong Zhong, is a Senior Experimentalist from Gannan Normal University. He graduated from Physics Education in Gannan Normal University in 1996 with the Bachelor of Science. His research interests include monolithic processor, computer network, security and encryption technology, database management, and computer applications. He has worked on computer-based system design and application for more than 20 years. He has published several papers in journal and international conferences.